

# Development of epoxy-based electrets

Yu-Cheng Liu · Yasuhiro Aoyagi · D. D. L. Chung

Received: 15 November 2007 / Accepted: 6 December 2007 / Published online: 11 January 2008  
© Springer Science+Business Media, LLC 2008

**Abstract** The use of a diepoxide resin in the form of 1,4-butanediol diglycidyl ether as the epoxy resin, lithium perchlorate (20 wt.%) as the ionic salt, a hardener (4,7,10-trioxatridecane-1,13-diamine, 15 wt.%) as the curing agent, and a poling DC electric field of 720 V/m gives an electret that exhibits a maximum voltage of 3.4 V during poling (30 min) and a stabilized voltage of 0.67 V after depoling (7.0 h). An epoxy system that hardens slowly (such as one with less hardener) is preferred, due to the longer time during poling for the ions to remain mobile. The rate of hardening rather than that of curing is the governing factor. The lithium salt hastens the curing, but it provides the ions and stabilizes the electret voltage, particularly during the first 30 min of depoling. After the first 30 min of depoling, crosslinking significantly enhances the stability of the electret voltage. The time constant for depoling is 0.8 h during the first 30 min of depoling and is 9 h afterward. Decrease of the lithium salt proportion from 20 to 10 wt.% still provides an effective electret, although the performance is reduced. An epoxy resin produced from Bisphenol F and epichlorohydrin is ineffective due to the high viscosity and fast hardening.

## Introduction

### Electrets

Electrets in the form of polymer films are commercially used in microphones [1–3]. This application is based on the

notion that the electret voltage is affected by the acoustic vibrations. Other applications of electrets include dust anchoring [4], blood platelet adhesion [5], memories [6], dosimetry of  $\gamma$ -radiation [7], and others [8].

The electret effect has been observed in polymers, particularly polyvinylidene fluoride [9–16], which is attractive for its polar bond and the consequent electric polarizability. It has also been observed in ceramics, particularly Pb(Ti, Zr)O<sub>3</sub> [17], CaTiO<sub>3</sub> [18], MgO–CaO–SiO<sub>2</sub>–Al<sub>2</sub>O<sub>3</sub> [19], and hydroxyapatite [20].

The electret behavior originates from a built-in voltage, which is stable and exists due to some form of prior poling or excitation. The poling involves the application of a voltage, which causes electric polarization, i.e., the separation of the positive and negative charge centers. This separation is due to the difference in the spatial distribution of the positive and negative charges in the material. Since the negative ions move toward the positive end of the applied electric field and the positive ions move toward the negative end of the applied electric field, the electric field resulting from the polarization opposes the applied electric field. The special aspect of the electret effect is that the charges associated with the polarization relax and form a core, which then induces surface charges of opposite sign. It is the surface charges that are responsible for the electret effect. Because the surface charge is opposite in sign from that associated with the polarization and the electret voltage is measured at the surface, the electret voltage polarity (Fig. 1) is opposite to the polarization voltage polarity (Fig. 2) and is same as the poling voltage polarity.

The charging of a polymer electret is conventionally achieved by the use of corona voltage application [21], electron beam bombardment [21, 22], and triboelectrification [23]. Corona methods are most common. In contrast, this paper investigates the use of poling during the curing of a thermosetting polymer resin. The poling involves DC

Y.-C. Liu · Y. Aoyagi · D. D. L. Chung (✉)  
Composite Materials Research Laboratory,  
University at Buffalo, State University of New York,  
Buffalo, NY 14260-4400, USA  
e-mail: ddchung@buffalo.edu  
URL: <http://alum.mit.edu/www/ddchung>

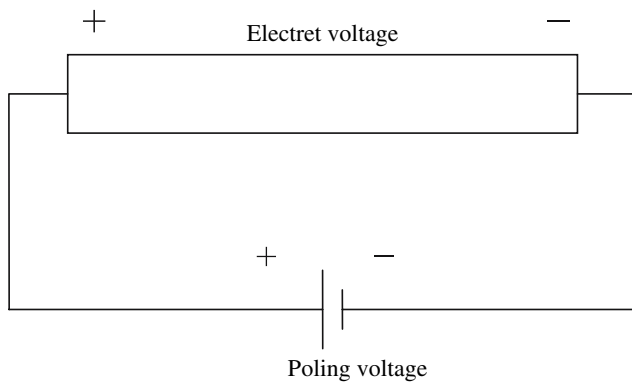


**Fig. 1** Illustration of the electret voltage polarity, which is same as the poling voltage polarity

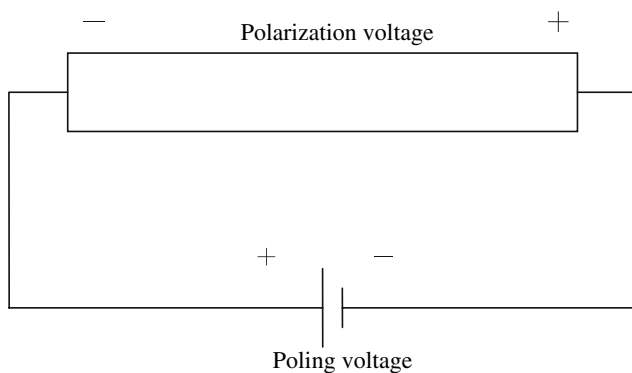


**Fig. 2** Illustration of the polarization voltage polarity, which is opposite to the poling voltage polarity

electric field application, which causes ions to move or polar bonds to rotate, thus resulting in polarization. PVDF is one of the most common electret polymers, due to the polar nature of some of the bonds there. In order to exploit the movement of ions as the mechanism of polarization, ions must be present. Polymers do not have ions, unless they are doped with ions, which can be provided by appropriate ionic salts.

Epoxy [24, 25] is the most common polymer matrix for structural composites, such as continuous carbon fiber composites that are used for lightweight structures. The use of a polymer matrix, that is an electret, is attractive for making a structural composite, so that the structural composite becomes multifunctional. An example of a nonstructural function that may be provided is strain sensing, since strain or vibration affects the electret voltage, which thus serves as an indicator of the strain. Such sensing is valuable for structures for the purpose of structural vibration control, load monitoring, and structural health monitoring.

Due to the importance of epoxy in composites, this article is focused on the development of epoxy-based

electrets. Epoxy resin is a thermosetting polymer, in contrast to the thermoplastic polymers in prior work on polymer electrets. Before the resin cures completely, the ions present are mobile and would move in response to an applied electric field. As the field is maintained throughout most of the curing process, the ions remain in the drifted position after curing, thus resulting in a built-in voltage in the cured polymer.

## Objectives

The objectives of this paper are (i) to fabricate epoxy-based electrets by poling during curing at room temperature, (ii) to formulate and characterize epoxy-based electrets, and (iii) to understand the relationships among electret formation, electret stability, and composition of epoxy–matrix electrets.

## Challenges

The main challenges related to the development of epoxy-based electrets are summarized below:

- (i) That the poling is conducted at room temperature means that the curing is also at room temperature, thus limiting the choice of epoxy systems.
- (ii) The ability of a salt to dissolve in an epoxy system limits the choice of the salt and the choice of the epoxy system. This ability depends on the backbone structure of the resin molecule and on the procedure of adding the salt to the system. For example, the salt may be added to either the resin or the curing agent. The heat generated by the dissolution may affect the curing reaction rate.
- (iii) The resin tends to become quite stiff in a short time, even though complete curing may take a relatively long time. As a consequence, the time period for the ions to drift during poling is limited.
- (iv) The electrical contacts used to conduct poling need to be a material that is nonreactive to the salt and other ingredients.

## Research approach

### Introduction

This article is an experimental investigation that is directed at developing epoxy-based electrets. These materials are epoxy systems with ionic doping. The dopant is a lithium salt, which provides lithium ions. Furthermore, the effect of

poling during curing on the electret and on the dielectric behavior is addressed. In addition, the effect of depoling is investigated.

The experimental approach involves the following aspects:

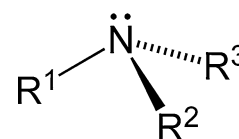
- (i) Epoxy systems (i.e., combinations of resin and curing agent) are assessed in terms of their suitability for doping and poling. Selection of the epoxy system is conducted by evaluation of the curing rate, the hardening rate, and the viscosity of the resin. All three quantities need to be sufficiently low in order for poling to be effective. The curing rate is assessed by calorimetric measurement of the heat of curing as curing progresses. The hardening rate is assessed by penetration testing as curing progresses.
- (ii) Formulations of epoxy system with salt doping are developed. The method of doping is also developed.
- (iii) Poling is conducted for various formulations, with the electret voltage monitored during poling. Poling occurs at room temperature and starts essentially when curing starts. The condition for attaining a high electret voltage is determined.
- (iv) The stability of the electret is investigated by measuring the voltage during depoling (immediately after poling) under an open-circuited condition. The depoling process is characterized in terms of the time constant of the process.
- (v) The doped epoxy systems with and without poling are characterized in terms of the relative dielectric constant, which is fundamental to the dielectric behavior and is a quantity that is affected by the ion concentration. The measurement is conducted at 1.0 MHz, using a parallel-plate capacitor geometry, in which the specimen is sandwiched by two copper plates.

## Epoxy

Epoxy is chosen as the polymer for this work due to its importance as the matrix of structural composites. The strong adhesiveness of epoxy stems from the polar bonds that the epoxy forms with the surface that it contacts. The polar bonds are attractive for electric polarization.

Epoxy or polyepoxide is a thermosetting epoxide polymer that cures (polymerizes and crosslinks) when it is mixed with a curing agent, also known as a hardener. An epoxy resin must be crosslinked in order to attain the desirable mechanical properties. When epoxy is mixed with an appropriate curing agent, the resulting reaction is exothermic. A curing agent typically has active hydrogen atoms attached to nitrogen, oxygen, or sulfur atoms. The

**Fig. 3** The general structure of an amine



reactive groups in the epoxy resin are mainly the terminal epoxide groups.

Amine-curing agents are the most common for epoxy formulations. Amines are organic compounds that contain nitrogen as the key atom, as illustrated in Fig. 3. Primary amines arise when one of the three hydrogen atoms in ammonia is replaced by an organic substituent; secondary amines have two organic substituents bound to nitrogen atoms, together with one hydrogen atom; and tertiary amines have all three hydrogen atoms replaced by organic substituents. Similarly, an organic compound with multiple amino groups is called a diamine, triamine, tetraamine, and so forth.

An amine-curing agent typically has more than three reactive sites per molecule. These sites facilitate the formation of a three-dimensional polymer network when the curing agent is mixed with the epoxy resin. The active hydrogen atom of the amine is what reacts with the epoxide group of the resin. The structure of the amine-containing organic compound and the number and type of amine groups in the compound govern the rate of crosslinking and the properties of the resulting polymer.

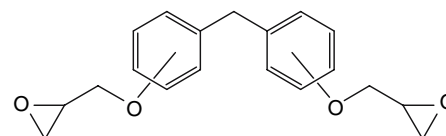
## Experimental methods

### Raw materials

Two types of epoxy resin (thermosetting) are used in this work: Epikote resin 862 (Table 1) and Heloxy epoxy functional modifier 67 (Table 2). Both are from Resolution Performance Products, Houston, TX. Both are chosen because of their low viscosity, though the viscosity of Heloxy 67 is much lower than that of the Epikote 862. In

**Table 1** Properties of Epikote resin 862

Epikote resin 862

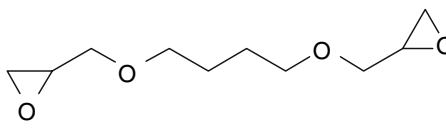


Epoxy equivalent weight 165–173 g

Viscosity at 25 °C 25–45 P

Density 1.17 g/cm<sup>3</sup>

**Table 2** Properties of Heloxy Modifier 67

Heloxy Modifier 67	
Epoxy equivalent weight	120–135 g
Viscosity, at 25 °C	0.13–0.18 P
Density	1.09–1.11 g/cm <sup>3</sup>
Boiling point	266 °C

Tables 1 and 2, the epoxy equivalent weight refers to the molecular weight divided by the number of epoxide groups in the molecule.

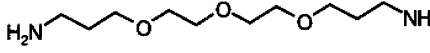
Epikote 862 is a low-viscosity epoxy resin produced from Bisphenol F and epichlorohydrin. It contains no diluent. Typical uses include compositions for the building and civil engineering industries, e.g., flooring compounds, adhesives, mortars, and grouts.

Heloxy 67 is a diepoxide resin in the form of 1,4-butanediol diglycidyl ether. It is conventionally used as a reactive diluent for reducing the viscosity of epoxy resins. The internal flexibility exhibited by this resins derives from the long aliphatic chain and the ether linkage in the chain.

The hardener (curing agent) used for either resin is 4,7,10-trioxatridecane-1,13-diamine from BASF Corporation, NJ. It is an etherdiamine in the form of a colorless liquid. The properties are shown in Table 3.

The lithium salt used for doping the polymer with ions was anhydrous lithium perchlorate (LiClO<sub>4</sub>), with melting point of 236 °C and density of 2.43 g/cm<sup>3</sup>, as provided by MP Biomedicals, Ohio. Lithium perchlorate is in the form of a white powder. It is special in that it exhibits high solubility in many solvents, including organic solvents. For example, its solubility in diethyl ether is 113.72 g/100 g (i.e., 53%) [26]. Lithium perchlorate has the highest oxygen content (by weight) of all the perchlorates. It is extensively used as an electrolyte in lithium batteries [27–29], as it does not undergo oxidation at the anode. In relation to epoxy, lithium perchlorate is particularly

**Table 3** Properties of 4,7,10-trioxatridecane-1,13-diamine (C<sub>10</sub>H<sub>24</sub>N<sub>2</sub>O<sub>3</sub>)

4,7,10-Trioxatridecane-1,13-diamine	
Molecular weight	220.3 g/mol
Melting point	–32 °C
Boiling point	146–148 °C (1 mbar)
Assay	min. 97%

attractive, because it promotes the opening of the epoxide groups in the epoxy resin, thereby catalyzing the curing reaction [26]. Potassium hydroxide (KOH), a more common salt, was found in this work to be insufficiently soluble in the epoxy resins, so it was not used in the investigation reported here.

### Materials processing

The polymers were fabricated by first grinding (by using a mortar and a pestle) the lithium salt to form a powder. The lithium salt could not be well dissolved in any of the resins, so it was necessary for it to be combined with the hardener rather than the resin. The hardener was mixed with the lithium salt and was stirred until all the lithium salt had been dissolved in the hardener. The alternate procedure of adding the salt to the resin prior to adding the hardener was found to fail, as it caused the curing reaction to increase suddenly, due to the heat generated by the dissolution of the lithium salt. The resin was added to the solution of the salt in the hardener. After this, the mixture was stirred for at least 5 min, until the mixture appeared uniform. The proportion of lithium salt was either 10% or 20% of the weight of the specimen. This proportion is below the solubility of 53% [26]. The dissolution, as expected, was complete. The entire procedure, including the curing, was carried out at room temperature.

The hardener proportion in phr (parts hardener per hundred parts of resin) was calculated using the equation

$$\text{Hardener phr} = \frac{\text{hardenerHEW} \times 100}{\text{Resin EEW}}, \quad (1)$$

where HEW (the hardener equivalent weight = 55 g) is the weight of the hardener (4,7,10-trioxatridecane-1,13-diamine) containing one mole of either amine hydrogen or anhydride, and EEW (the epoxy equivalent weight) is the weight of the resin containing one mole of epoxide groups (EEW = 120–135 g for Heloxy Modifier 67, EEW = 165–173 g for Epikote resin 862). The values of the hardener proportion in phr for the two epoxy resins are shown in Table 4.

**Table 4** The proportion of the hardener used with the epoxy resin, according to Eq. 1

Epoxy resin type	Hardener phr	LiClO <sub>4</sub> (wt.%)	Hardener (wt.%)
Heloxy <sup>a</sup>	43.14	0	30.0
Heloxy <sup>a</sup>	43.14	10	27.0
Heloxy <sup>a</sup>	43.14	20	24.0
Epikote resin 862	32.54	10	22.5

<sup>a</sup> Heloxy Modifier 67

Unless noted otherwise, the weight of the hardener relative to the weight of the specimen is as shown in the last column of Table 4, as calculated from the hardener proportion in phr. For Heloxy 67 with 10 wt.% lithium perchlorate, the hardener proportion was, in some cases, reduced from 27 wt.% to 16.5 wt.% in order to slow down the curing reaction. For Heloxy 67 with 20 wt.% lithium perchlorate, the hardener proportion was, in some cases, reduced from 24 wt.% to 15 wt.% in order to slow down the curing reaction.

### Electric poling and depoling

Electric poling is well known in case of ferroelectric materials, in which ferroelectric domains are aligned to produce a useful electroactive material that exhibits a net macroscopic polarization. For the case of polymers, the poling is often conducted by corona charging after the completion of polymerization or curing [30]. Corona charging requires a high electric field (e.g.,  $5 \times 10^6$  V/m [31]). In contrast, poling is conducted in this work by application of a low electric field (720 V/m) during curing. A low electric field is associated with low cost and implementations simplification.

The lithium-doped resin prepared using the procedure mentioned in section “Materials processing” was poured into a silicone mold (60 mm long, 10 mm wide, and 1 mm deep). Bundles of carbon fiber were placed in the resin for the purpose of electric field application and/or voltage measurement. Carbon fiber rather than metal wire was used due to the chemical inertness of carbon. Each bundle extended along the entire 10-mm width of the mold cavity. The portion of each bundle that was in contact with the resin was immersed in the resin. Unless noted otherwise, each of the two bundles was used for both electric field application and voltage measurement. The field application was continuous, except for interruption by periods of 3 s each for the purpose of voltage measurement. For investigating the potential distribution along the length of the specimen, two additional bundles of carbon fiber were placed, so that there were a total of four bundles, as shown in Fig. 4. The inner two bundles were only for voltage measurement.

The carbon fiber was Thornel P-100 mesophase-pitch-based carbon fiber provided by BP Amoco Performance Products, Inc., Alpharetta, GA. This type of carbon fiber is chosen because of its high degree of graphitization and the consequent low electrical resistivity. Such fiber is used for the negative electrode of secondary batteries [32]. The carbon fiber used in this work has diameter: 10  $\mu\text{m}$ , density: 2.13  $\text{g/cm}^3$ , electrical resistivity:  $10^{-3}$   $\Omega$  cm, tensile modulus: 760 GPa, tensile strength: 2,400 MPa, and

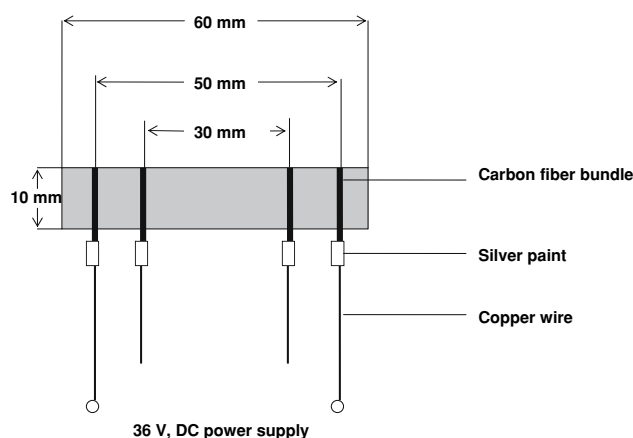


**Fig. 4** Specimen configuration. The shaded region is the resin contained in a mold cavity of size  $60 \times 10 \times 1.0$  mm

elongation at break: 0.3%. Each bundle that constitutes an electrical contact contained about 150 fibers and weighed 0.25 mg. The width (along the 60-mm length of the mold cavity) of each electrical contact was  $0.8 \pm 0.2$  mm.

Each electrical contact was connected to a copper wire using silver conductive paint. The silver paint joint was located outside the mold cavity. A DC power supply (Harrison 6294A DC power supply, Hewlett-Packard Development Co., Houston, TX) was used to apply a constant voltage of 36 V (electric field of 720 V/m) through the two outer electrical contacts for a period of 12 h.

In order to investigate the stability of the electret formed during poling, depoling was allowed to occur in the absence of an applied electric field under an open-circuited condition. The depoling was initiated immediately after various times of poling (i.e., 0.5, 1.0, 2.0, 5.0, and 12 h). The voltage at the two contacts (the outer two contacts in case four contacts were present) was monitored continuously during depoling. The voltage was continuously measured by using a Keithley 2001 multimeter (Keithley Instruments Inc., Cleveland, OH).

Table 5 lists the combinations of composition and poling condition investigated. Each combination is referred to as a specimen type, which is designated A, B, ..., and I. The poling electric field, if present, was 720 V/m. The compositions of specimen types A, B, C, and D were designed according to Eq. (1). The hardener proportions of specimen types E, F, and G were below those obtained by using Eq. (1), in order to slow down the curing reaction. The various compositions differ in one or more of the following parameters: the choice of epoxy resin (either Heloxy Modifier 67 or Epikote resin 862), lithium salt proportion (63.0, 66.0, 67.5, 70.0, or 73.5 wt.%), and hardener proportion (15.0, 16.5, 22.5, 27.0, or 30.0 wt.%).



**Table 5** The combinations of composition and poling condition investigated

Specimen type	Epoxy type	Epoxy (wt. %)	LiClO <sub>4</sub> (wt. %)	Hardener (wt. %)	Hardener phr	Poling electric field (V/m)
A	Heloxy <sup>a</sup>	70.0	0	30.0	43	0
B	Heloxy <sup>a</sup>	63.0	10	27.0	43	0
C	Heloxy <sup>a</sup>	70.0	0	30.0	43	720
D	Heloxy <sup>a</sup>	63.0	10	27.0	43	720
E	Heloxy <sup>a</sup>	73.5	10	16.5	23	0
F	Heloxy <sup>a</sup>	73.5	10	16.5	23	720
G	Heloxy <sup>a</sup>	65.0	20	15.0	23	720
H	Epikote <sup>b</sup>	67.5	10	22.5	33	0
I	Epikote <sup>b</sup>	67.5	10	22.5	33	720

Each combination is referred to as a specimen type

<sup>a</sup> Heloxy Modifier 67

<sup>b</sup> Epikote resin 862

### Testing methods

**Epoxy curing monitoring.** The curing of epoxy systems was monitored by the use of differential scanning calorimetry (DSC) in order to measure the heat of reaction as a function of time during the reaction. Since the reaction is exothermic, the heat evolved is monitored as a function of time at a constant temperature (room temperature, around 25 °C). An aluminum DSC sample pan was used in conjunction with a Perkin-Elmer Corp. (Norwalk, CT) DSC7 instrument. The mass of each specimen was  $10.00 \pm 0.25$  mg.

After preparing a specimen by mixing the various ingredients, the specimen was immediately placed in the DSC sample pan and the heat flow measurement was then immediately started. However, there was a time gap of approximately 10 min between the start of mixing and the start of the DSC measurement. As a consequence, the DSC measurement did not commence at the start of the curing reaction.

**Epoxy hardening monitoring.** Various forms of penetrating testing are used in the industry to measure the consistency of lubricating greases, oils, and related materials. This test involves the penetration of the medium under examination by a standardized penetrator and measurement of the extent of penetration. This test is adapted in this work for monitoring the process of epoxy hardening, as the extent of penetration decreases as the epoxy hardens.

Figure 5 illustrates the penetration testing instrument, which is a gravity-penetrometer based on ASTM D 1321-97. The penetrator (a 15-5 precipitation-hardened stainless steel rod of diameter 0.51 mm, length 195 mm, and mass 0.33 g) was precisely lowered to the surface of the paste under test. Then it was allowed to sink into the paste by its own weight during a particular duration of testing (5.0 s in this work). The penetration was indicated by the extent of vertical movement of the penetrator, as measured by

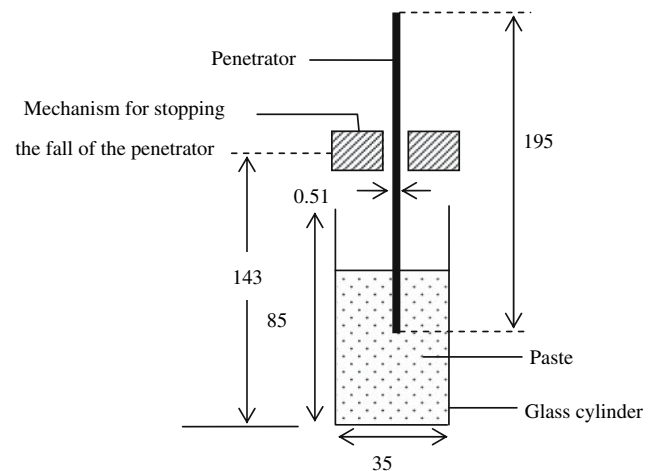


**Fig. 5** Penetration testing set-up. All dimensions are in mm

calipers. The instrument in this work used a timer to control the test duration of 5.0 s. A solenoid connected to the timer was used to activate a simple mechanism for stopping the fall of the penetrator exactly at the end of 5.0 s. Each specimen was tested for three times. The depth of each specimen was  $28 \pm 1$  mm.

**Relative dielectric constant measurement.** The relative dielectric constant  $\kappa$  is the ratio of the permittivity of a material,  $\epsilon$ , to the permittivity of free space,  $\epsilon_0$  (equal to  $8.854 \times 10^{-12}$  C/V m), i.e.,

$$\kappa = \epsilon/\epsilon_0.$$

In this work, the relative dielectric constant  $\kappa$  is measured for polymers with and without lithium doping, and with and without poling, in order to investigate the effects of the doping and of the poling on the dielectric behavior of the polymer. All specimens were tested after the completion of 13 h of poling and a subsequent period of at least 150 h in the absence of a poling voltage

(open-circuited condition), in order to investigate the behavior of the stable electret.

The specimen was of size  $25 \times 10 \times 1.0$  mm, as obtained by cutting the specimen illustrated in Fig. 4, so as to use the 25-mm long central part of the specimen away from the electrical contacts. It was sandwiched by copper plates to form a parallel-plate capacitor configuration. During testing, the sandwiched was compressed in the direction perpendicular to the plane of the sandwich at a pressure of 1.68 kPa. The copper plates ( $25 \times 10 \times 3.1$  mm), which had been mechanically polished with alumina particles of size 0.3  $\mu\text{m}$ , served as electrodes. The impedance was measured along the direction of poling by using the two-probe method and a capacitance meter (HP 4280A, Hewlett Packard Corp., Houston, TX). The magnitude of the AC voltage used in the measurement was 0.5 V (i.e., electric field = 0.5 V/mm). The frequencies used were 1.0 MHz. The dielectric constant was calculated from the capacitance and the specimen dimensions, i.e.,

$$\kappa = C\ell/(\varepsilon_0 A),$$

where  $C$  is the capacitance,  $\ell$  is the thickness of the specimen, and  $A$  is the area of the specimen in the plane of the sandwich.

**DC electrical resistivity measurement.** The DC electrical resistivity was measured during natural depoling (conducted in the absence of an applied electric field in an open-circuited condition), which was initiated immediately after poling at 720 V/m for 30 min. Due to the high values of the resistance, the two-probe method was used. In this method, each of the two electrical contacts was used for both voltage measurement and current application. The contact configuration and materials are as described in Fig. 4, except that only the two outer contacts in Fig. 4 were used. For specimens of resistance less than 10 M $\Omega$ , the resistance was measured by using a current source to pass a current to the specimen that was in series with a 50  $\Omega$  resistor. For specimens of higher resistance, the resistance was measured by using a voltage source to pass a current to the specimen that was in series with a 1.0 M $\Omega$  resistor.

The resistance was measured in either the longitudinal direction or the through-thickness direction. The longitudinal direction was the poling direction, which was along the length of the specimen. The through-thickness direction was perpendicular to the plane of the specimen. In case of longitudinal resistance measurement, the electrical contacts were in the form of strips in the plane of the specimen, such that each strip was perpendicular to the length of the specimen. These were the same contacts that were used for poling. In case of through-thickness measurement, the electrical contacts were on the two opposite in-plane surfaces, such that the specimen excluded (by cutting) the

portions that were in the vicinity of the electrical contacts used for poling.

**RC time constant.** In an RC circuit, the time required to charge the capacitor through the resistor to 63.2% (i.e.,  $1 - e^{-1}$ ) of the full charge or to discharge it to 36.8% (i.e.,  $e^{-1}$ ) of its initial voltage is the time  $\tau$ , which is known as the RC time constant. In other words,

$$\tau = RC,$$

where  $R$  is the resistance in ohms and  $C$  is the capacitance in farads.

In this work, the RC time constant was calculated by using the resistance (measured using the method described in section “DC electrical resistivity measurement”) and the capacitance (measured using the method described in section “Relative dielectric constant measurement”) of specimens of size  $25 \times 10 \times 1.0$  mm in the direction of the 1.0-mm thickness.

## Results and discussion

Relative dielectric constant, electrical resistivity, and RC time constant

Table 6 lists the measured values of the relative dielectric constant (1.0 MHz) and of the DC electrical resistivity, along with the RC time constant calculated from them. In obtaining the RC time constant, it is more proper if both dielectric constant and resistivity are at the same frequency. The resistivity is expected to increase with increasing frequency, due to the skin effect, while the relative dielectric constant is expected to increase with decreasing frequency, due to dipole friction. Thus, with

**Table 6** Relative dielectric constant, electrical resistivity, and RC time constant of different types of specimen

Specimen type	Relative dielectric constant	Electrical resistivity ( $\Omega$ cm)	RC time constant ( $\mu\text{s}$ )
A	9.67 <sup>a,d</sup>	/	/
B	7.36 <sup>a,d</sup>	$5.5 \times 10^{6b,d}$	90 <sup>d</sup>
C	8.99 <sup>a,d</sup>	/	/
D	5.93 <sup>a,d</sup>	$1.6 \times 10^{7b,d}$	210 <sup>d</sup>
F	/	$2.6 \times 10^{4c,e}$	/
G	/	$1.0 \times 10^{4c,e}$	/

The specimen type designations are as explained in Table 5

<sup>a</sup> Polled for 10 h, followed by natural depolarization for 5 days

<sup>b</sup> Polled for 10 h, followed by natural depolarization for 10 days

<sup>c</sup> Polled for 30 min, followed by natural depolarization for 20 h

<sup>d</sup> Through-thickness direction

<sup>e</sup> Longitudinal (poling, in-plane) direction

both the resistivity and the relative dielectric constant at the same frequency (one between DC and 1.0 MHz), the RC time constant is expected to be higher than the values in Table 6. In other words, the time constant values in Table 6 can be considered as lower bound values.

The addition of the lithium salt decreases the relative dielectric constant, as shown by comparing the values for specimen types A and B (which have not been poled and have similar values of the hardener proportion) and by comparing those for specimen types C and D (which have been poled and have similar values of the hardener proportion). The decrease in the relative dielectric constant upon addition of the salt is attributed to the hastening of the curing reaction by the salt, as shown by calorimetry (section “Curing monitoring”). In other words, the salt does not merely provide ions, which would tend to increase the relative dielectric constant, in contrast to the decrease observed.

Comparison of the results for specimen type B (without poling) and specimen type D (with poling) in Table 6 shows that poling decreases the relative dielectric constant and increases both the resistivity and the RC time constant. All three properties are in the through-thickness direction. These effects are all due to the gathering of the ions in the vicinity of the electrodes (particularly the cathode, toward which the lithium ions drift) and that these areas have been cut off prior to the measurement of the relative dielectric constant or resistivity in the through-thickness direction. Without poling, the ions are uniformly distributed; after poling, they are not. As a consequence, the tested area of the specimen has a lower ion concentration after poling.

That poling decreases the relative dielectric constant in the through-thickness direction is also shown in Table 6 by comparing specimen types A and C (which have the same composition) and comparing specimen types B and D (which have the same composition). The effect of the poling on the relative dielectric constant is less than that of the salt.

Curing monitoring

Figures 6 and 7 show the heat flow vs. time during the curing of specimen types A, B, E, G, and H. Figure 7 is a magnified version of the part of Fig. 6 up to a time of 300 min. In each figure, the exothermic direction is the downward direction of the vertical axis. Since no DSC measurement was made in the beginning of the curing reaction time period, the initial part of the curve of heat flow vs. time corresponding to the heat evolved increasing with time is absent, except for specimen type A, the curing of which is slowest among the four specimen types studied. The leveling off of the curve indicates the completion of

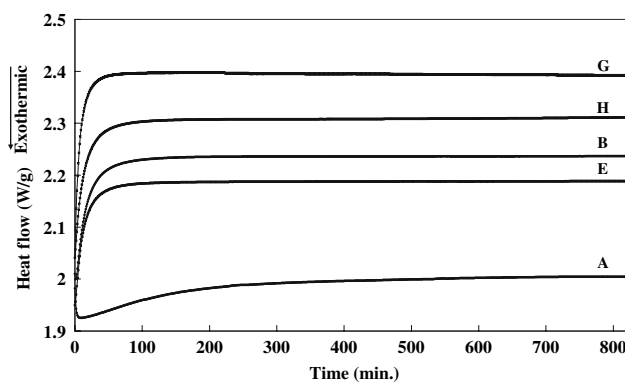


Fig. 6 The variation of the heat flow with time up to 800 min for specimen types A, B, E, G, and H

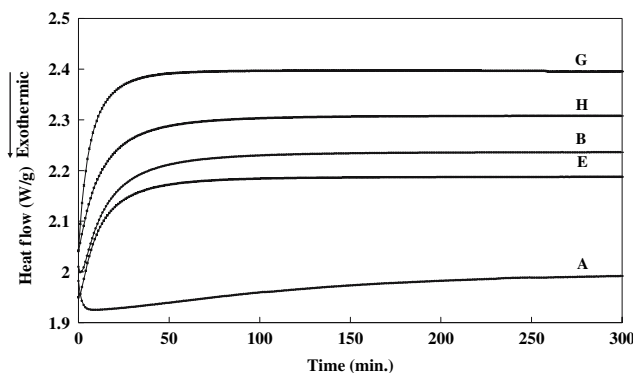


Fig. 7 The variation of the heat flow with time up to 300 min for specimen types A, B, E, G, and H. This figure is a magnified version of a part of Fig. 6

the curing reaction. The area above each curve and below the horizontal line corresponding to the leveling off indicates the heat evolved during the part of the curing reaction that was monitored. The time for the completion of curing is taken as the time at which the DSC curve starts to level off. This time is shown in Table 7.

Curing takes longer for specimen type A than specimen type B (Table 7) because of the presence of lithium salt in B and the absence of lithium salt in A. In spite of the higher hardener concentration in A than B, the absence of lithium

Table 7 The time for curing completion (based on DSC results) for the various types of specimen

Specimen type	Time for completion of curing (min)
A	800 ± 25
B	200 ± 25
E	200 ± 25
G	100 ± 25
H	200 ± 25

Refer to Table 5 for explanation of the specimen type designations



salt makes the curing slow for A. Both specimen types B and E contain 10 wt.% lithium salt. Curing takes similar times for specimen types B and E, in spite of the higher hardener concentration in specimen B. Specimen type G contains 20 wt.% lithium salt. Curing is faster for specimen type G than specimen types B and E because of the higher lithium salt content in G. These observations suggest that the lithium salt affects the curing rate more than the hardener concentration.

Curing is slower for specimen type H than the other types listed in Table 7, in spite of the lithium salt present and the substantial hardener concentration in specimen type H. This slowness is attributed to the type of epoxy resin in specimen type H.

### Hardening monitoring

Figure 8 shows the variation of the depth of penetration with time from mixing (i.e., specimen preparation by mixing the various ingredients) for specimen types B, C, E, and G. The penetration depth decreases with time due to the hardening that accompanies the curing. The time at which the penetration depth reaches zero is taken as the time for the completion of hardening. This time is listed in Table 8 for the four specimen types.

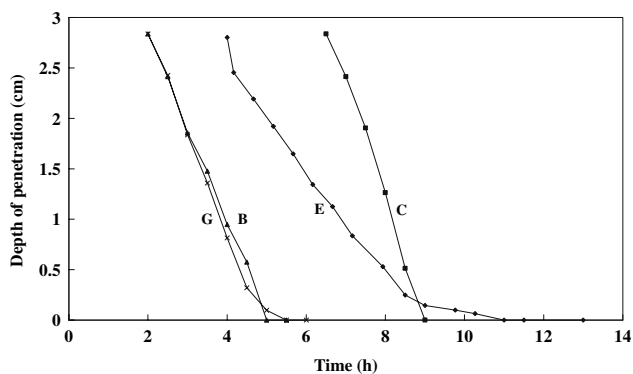


**Fig. 8** The variation of the depth of penetration with time from mixing for specimen types B, C, E, and G

**Table 8** The time for hardening completion for various specimen types

Specimen type	Time for hardening completion (h)
A	$9.0 \pm 0.5$
B	$5.0 \pm 0.5$
E	$11.0 \pm 0.5$
G	$5.5 \pm 0.5$

Refer to Table 5 for explanation of the specimen type designations

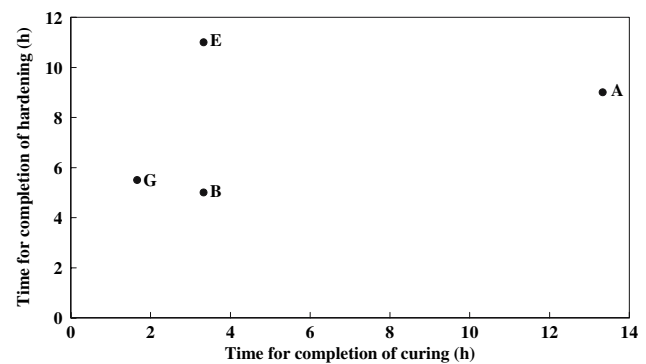


**Fig. 9** Time for completion of hardening vs. time for completion of curing for various specimen types

During the first 2.0–6.5 h (depending on the specimen type) after mixing, the viscosity is so low that the penetrator hits the bottom of the specimen container, thus resulting in no meaningful measurement of the depth of penetration. Therefore, Fig. 8 does not show the depth of penetration for the entire time range from zero time onward.

Figure 9 shows that there is no correlation between the time for completion of hardening (based on penetration testing) and the time for completion of curing (based on DSC, section “Curing monitoring”). A long time of hardening allows the ions to drift in response to the applied electric field for a long time, so the hardening time matters more to poling than the curing time does.

### Electret formation

Table 9 shows the measured voltage at the outer contacts as a function of the poling time. For each specimen type, the voltage increases with the poling time, due to poling. However, it decreases with increasing poling time beyond a particular poling time, as shown in Fig. 10, due to the natural depoling that occurs during the poling interruptions associated with the 3-s periods of voltage measurement. As the resin hardens over time, poling becomes more and more inefficient. Therefore, poling subsequent to an interruption is unable to restore the polarization to the level prior to the interruption after the hardening has reached a certain level. As a consequence, the measured voltage decreases with poling time after the hardening has reached a certain level.

As shown in Fig. 10 and Table 10, the voltage stabilizes as poling occurs, due to the accompanying curing. By 12 h of poling, specimen types C and D essentially attain stability in the voltage, while specimen types F and G have not yet attained stability. That specimen types F and G take longer times for the voltage to stabilize relates to the relatively small extent of voltage decrease after the maximum

**Table 9** The variation of the measured voltage (at the outer contacts) with the poling time for each of five specimen types (C, D, F, G, and I)

Poling time	Voltage (V)				
	C	D	F	G	I
10 min	0.72	2.98	3.03	3.36	1.04
20 min	0.78	3.30	3.13	3.42	0.58
30 min	0.87	3.32	3.15	3.41	0.27
40 min	0.90	3.28	3.16	3.38	0.10
50 min	0.94	3.27	3.15	3.35	0.04
1.0 h	0.94	3.22	3.15	3.33	0.02
2.0 h	0.91	2.78	3.12	3.30	0.01
3.0 h	0.74	2.36	3.10	3.26	0.006
4.0 h	0.56	2.06	3.01	3.21	0.008
5.0 h	0.42	1.85	2.94	3.14	0.005
6.0 h	0.29	1.65	2.90	3.01	0.003
7.0 h	0.21	1.46	2.84	2.89	0.002
8.0 h	0.18	1.34	2.78	2.81	0.006
9.0 h	0.15	1.25	2.67	2.72	0.001
10 h	0.12	1.19	2.59	2.63	0.001
11 h	0.09	1.19	2.42	2.50	0.001
12 h	0.08	1.16	2.29	2.45	0.001

Refer to Table 5 for explanation of the specimen type designations

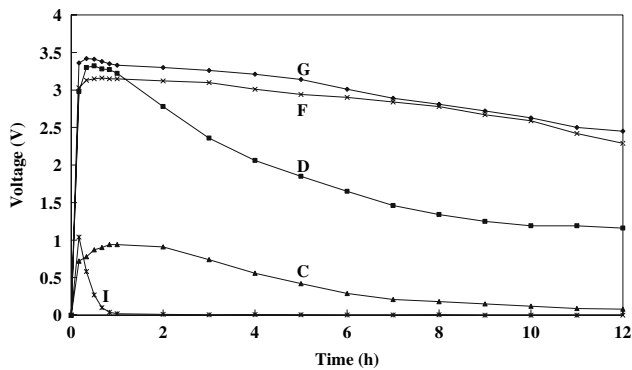


**Fig. 10** The variation of the voltage for the outer contacts with the time from the start of voltage application for all specimen types. It takes less than 3 min from the completion of mixing to the start of voltage application

voltage has been attained. This means that specimen types F and G are particularly attractive for the formation of a stable and significant electret. This behavior of specimen types F and G is attributed to the combination of lithium salt’s presence and low hardener proportion. In contrast, specimen types C and D have higher hardener proportions. In addition, specimen type C has no lithium salt. Specimen type I is the least attractive among the various specimen types shown in Table 10, because of the Epikote resin 862, which cures fast and has a high viscosity compared to the Heloxy Modifier 67 epoxy resin.

The maximum voltage for each curve in Fig. 10 relates to the maximum voltage that can be attained during poling. Among the specimen types in Table 10, specimen type G gives the highest value of the maximum voltage. Specimen type D attains almost as high a value of the maximum voltage, but it suffers from a relatively low value of the stabilized voltage (Table 10). The superior performance of specimen type G is attributed to the combination of high lithium salt content (20 wt.%) and low hardener content. In contrast, specimen type C is inferior to the other types in Table 10 that involve the same epoxy resin (i.e., types D, F, and G), because of the absence of lithium salt and the high hardener content.

The time for attaining the maximum voltage attained during poling is shown in Fig. 11 to correlate to a limited

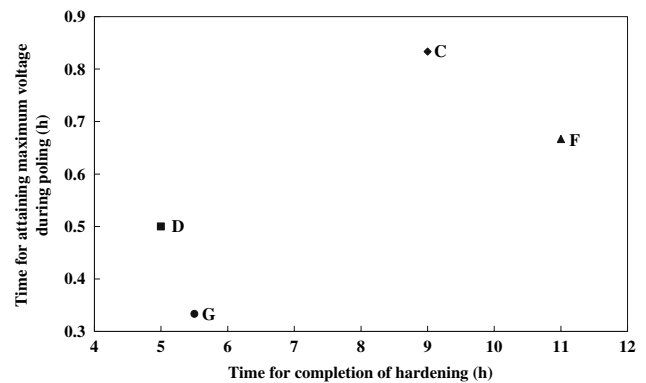


**Fig. 11** The time for attaining the maximum voltage during poling vs. the time for completion of hardening

**Table 10** Stabilized voltage (outer voltage) relative to the maximum voltage (outer voltage) during poling

	Specimen type				
	C	D	F	G	I
Stabilized voltage (V)	<0.080	<1.160	<2.290	<2.450	<0.001
Maximum voltage (V)	0.940	3.320	3.160	3.420	1.040
The ratio of the stabilized to maximum voltage	0.085	0.349	0.724	0.716	0.00096

In case that the voltage does not attain complete stabilization by 12 h, the voltage at 12 h is taken to be the upper bound of the stabilized voltage (Fig. 10)

**Table 11** Comparison of the voltage at the outer and inner electrical contacts during poling

Poling time (h)	Voltage (V)									
	Specimen type C		Specimen type D		Specimen type F		Specimen type G		Specimen type I	
	Outer	Inner	Outer	Inner	Outer	Inner	Outer	Inner	Outer	Inner
1.0	0.94	0.040	3.22	0.1800	3.15	−0.16	3.33	0.085	0.020	0.0035
2.0	0.91	0.045	2.78	0.0700	3.12	−0.20	3.30	0.080	0.010	0.0010
3.0	0.74	0.070	2.36	0.0100	3.10	−0.20	3.26	0.050	0.006	0.0030

Refer to Table 5 for explanation of the specimen type designations

degree with the time of completion of hardening (Table 8). This means that slow hardening is indeed favorable for extending the time that poling is effective during curing.

For any of the specimen types at any given time during poling, the voltage at the inner electrical contacts is much smaller than that at the outer contacts, as shown in Table 11 for three poling times. This means that, during poling, the potential does not drop linearly from one outer contact to the other outer contact. Rather, potential drop mainly occurs in the region near each of the two outer contacts. This is attributed to the drift of the ions toward the outer contacts in response to the applied electric field. The drift results in a relatively low concentration of ions in the part of the specimen between the inner contacts. This result is consistent with the observation that poling decreases the relative dielectric constant in the part of the specimen between the inner contacts (section “Relative dielectric constant, electrical conductivity, and RC time constant”).

The voltage obtained by using the outer contacts was obtained on specimens with and without the inner contacts. It was thus found that the voltage obtained by the outer contacts is not affected by the presence of the inner contacts.

### Depoling behavior

After a selected time period of poling, a specimen is allowed to depole naturally (in the absence of an applied electric field under an open-circuited condition) for the purpose of investigating the stability of the electret formed by the poling. Figure 12 and Tables 12 and 13 show the decay of the voltage during the depoling for various specimen types that have undergone prior poling for 30 min. Among specimen types C, D, F, and G, depoling is slowest for G and the stabilized voltage during depoling is highest for G. This is consistent with the strongest electret behavior observed in G during poling (Table 10). Among these specimen types, depoling is fastest and the stabilized voltage is lowest for C. This is consistent with the poorest electret behavior observed for C during poling (Table 10).

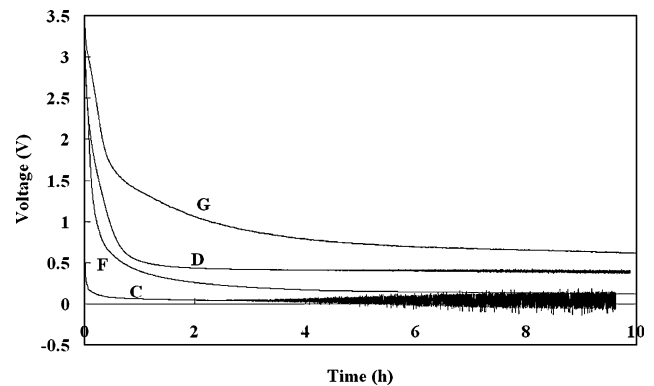


**Fig. 12** Variation of the voltage with time during depoling for specimen types C, D, F, and G, which have undergone immediately prior poling for 30 min

**Table 12** The stabilized voltage during depoling and the time for attaining the stabilized voltage for the case of 30 min of immediately prior poling

Specimen type	Time for stabilization (h)	Stabilized voltage (V)
C	1.0 ± 0.5	0.06 ± 0.01
D	2.0 ± 0.5	0.43 ± 0.01
F	5.0 ± 0.5	0.15 ± 0.01
G	7.0 ± 0.5	0.67 ± 0.01

Refer to Table 5 for explanation of the specimen type designations

**Table 13** Fractional decrease in voltage at various times of depoling (30 min to 2 h) for 30 min of immediately prior poling

Specimen type	Fractional decrease in voltage during depoling (V)			
	30 min	2.0 h	5.0 h	12 h
C	0.92	0.95	0.96	0.98
D	0.73	0.87	0.88	0.88
F	0.82	0.92	0.95	0.96
G	0.54	0.71	0.80	0.82

Refer to Table 5 for explanation of the specimen type designations

The increase in noise as time progresses for specimen type C (Fig. 12) is due to the increase of the electrical resistivity as time progresses. A high resistance causes

noise in the voltage reading provided by the multimeter. The increase in resistivity with time is due to the curing that continues to occur, since the poling time prior to depoling is just 30 min and curing is far from completion at the end of 30 min. The data for specimen type I is not included in Fig. 12, because the resistance is high and the voltage is noisy (even more noisy than for specimen type C) from the start of depoling.

The extent of prior poling affects the depoling. Figure 13 shows that the stabilized voltage during depoling increases with increasing time of prior poling. Table 14 shows that the fractional decrease in voltage at a given time of depoling tends to decrease with increasing prior poling time. This trend is clear for a depoling time of 2.0 h, although it is less clear for shorter depoling times. This trend is because of the curing that occurs during poling, so that a longer prior poling time corresponds to a longer curing time. The greater is the extent of curing, the lesser is the tendency to depole.

For all the specimen types and all the different times of prior poling, the time of depoling (Figs. 12 and 13) is much longer (by orders of magnitude) than the RC time constant (Table 6). This means that the electret is much more stable than what is expected for an equivalent RC circuit.

The time constant  $\beta$  of the depoling process can be obtained by applying the following equation to the data in Figs. 12 and 13.

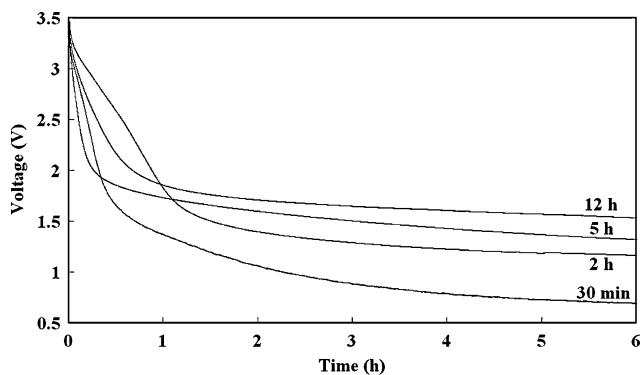


**Fig. 13** Variation of the voltage with time during depoling for specimen type G after different times of immediately prior poling

**Table 14** Fractional decrease in voltage at various times of depoling (30 min to 2 h) for specimen type G and various time periods (30 min to 12 h) of prior poling

Prior poling time	Fractional decrease in voltage during depoling (V)		
	30 min	1.0 h	2.0 h
30 min	0.54	0.62	0.71
2.0 h	0.30	0.51	0.62
5.0 h	0.49	0.52	0.56
12 h	0.39	0.48	0.52

$$V = V_0 \exp(-t/\beta),$$

where  $V$  is the voltage at time  $t$  and  $V_0$  is the voltage at  $t = 0$ . This equation means that  $\log(V/V_0)$  is linearly related to  $t$ , with a negative slope that relates to the reciprocal of  $\beta$ . Such a semi-logarithmic plot using the data of Fig. 12 is shown in Fig. 14. The plots in Fig. 14 are not linear, but each plot may be approximated as two linear segments of two different slopes, as shown by the straight lines in Fig. 14. The  $\beta$  values obtained from these slopes are listed in Table 15. The segment at earlier times is referred to as Period i; that at later times is referred to as Period ii. For each of the specimen types, the  $\beta$  value for Period i is lower than that of the corresponding Period ii. This means that the mechanism for the two periods are different. Among the specimen types shown in Table 15, the  $\beta$  value of Period i is highest for specimen type G and that of Period ii is highest for specimen type D. Specimen type G has a higher lithium salt content than specimen type F or D. Thus, a high lithium salt content probably contributes to causing the large  $\beta$  value for specimen type G in Period i through stabilizing the electrets, in spite of the small size of the lithium ions and the associated limited tendency to be held in place after poling. On the other

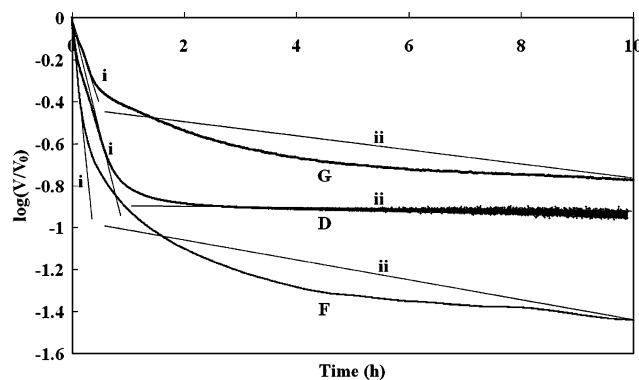


**Fig. 14** Plot of  $\log(V/V_0)$  vs. time corresponding to the data in Fig. 12. The slopes for two portions of each curve are shown and labeled i and ii

**Table 15** Time constant  $\beta$  for each of two time periods of depoling for specimen types D, F, and G

Specimen type	Time constant (h)	
	Period i	Period ii
D	$0.52 \pm 0.05$	$106 \pm 5$
F	$0.24 \pm 0.05$	$12 \pm 5$
G	$0.80 \pm 0.05$	$9 \pm 5$

The time of immediately prior poling is 30 min. Refer to Table 5 for explanation of the specimen type designations

hand, the  $\beta$  value for Period ii is highest for specimen type D, which distinguishes from specimen types G and F in its high hardener proportion. Thus, a high hardener content probably contributes to causing the large  $\beta$  value for specimen type D in Period ii through promotion of crosslinking. In other words, depoling in the early stage (Period i) is slowed down by the lithium salt, whereas depoling in the later stage (Period ii) is slowed down by the crosslinking.

The  $\beta$  value increases with the prior poling time, as shown for Period ii in the case of specimen type G (Fig. 15 and Table 16). This means that depoling in the later stage is slowed down by increasing the prior poling time, which relates to the curing time. Thus, depoling is slowed down by increased crosslinking, as indicated also by the data in Table 15. However, in Period i for specimen type G, there is no systematic relationship between the  $\beta$  value and the prior poling time (Table 16), due to the dominance of the lithium salt rather than the extent of curing in governing the  $\beta$  value in Period i, as mentioned above in relation to Table 15. The  $\beta$  value of 9 h for specimen type G in Period ii (Table 15) is similar to the value of 8.6 h (31,000 s) reported for PVDF [33].

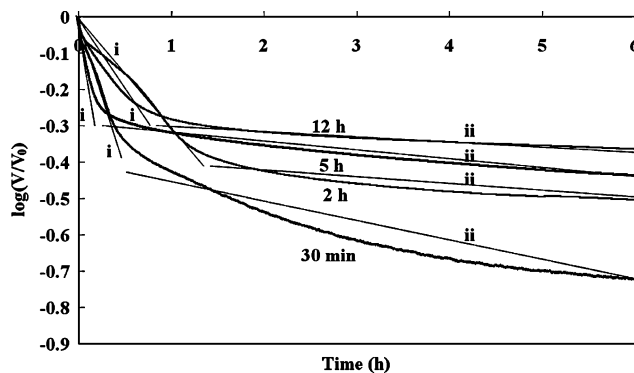


**Fig. 15** Plot of  $\log(V/V_0)$  vs. time corresponding to the data in Fig. 13. The slopes for two portions of each curve are shown and labeled i and ii

**Table 16** Time constant  $\beta$  for each of two time periods of depoling for specimen type G after different times of immediately prior poling

Prior poling time	Time constant (h)	
	Period i	Period ii
30 min	$0.80 \pm 0.05$	$9 \pm 5$
2.0 h	$2.00 \pm 0.05$	$14 \pm 5$
5.0 h	$0.60 \pm 0.05$	$22 \pm 5$
12 h	$1.30 \pm 0.05$	$40 \pm 5$

## Conclusion

Epoxy-based electrets have been developed in this work. The use of Heloxy Modifier 67 (a diepoxide resin in the form of 1,4-butanediol diglycidyl ether) as the epoxy resin, lithium perchlorate in the amount of 20 wt.%, a hardener (4,7,10-trioxatridecane-1,13-diamine) in the amount of 15 wt.% as a curing agent, and a poling electric field of 720 V/m results in an electret that exhibits maximum voltage of 3.4 V in the poling direction during poling (30 min) and stabilized voltage of 0.67 V after depoling (7.0 h). An epoxy system that hardens slowly (such as the one with a lower proportion of the hardener) is preferred for forming an electret, due to the longer time during poling for the ions to remain high in mobility. The rate of hardening rather than the rate of curing is the governing factor. The lithium salt hastens the curing, but it provides the necessary ions and stabilizes the electret voltage, particularly during the first 30 min of depoling. After the first 30 min of depoling, crosslinking becomes a significant mechanism for enhancing the stability of the electret voltage. The time constant for depoling is 0.8 h during the first 30 min of depoling and is 9 h after the first 30 min. Decrease of the lithium salt proportion from 20 to 10 wt.% still provides an effective electret, although the performance of the electret is reduced. Epikote 862 (a relatively low-viscosity epoxy resin produced from Bisphenol F and epichlorohydrin) is ineffective for providing epoxy-based electrets, due to the high viscosity (still too high) and fast hardening.

Future work should be directed toward further improvement of the formulation of the epoxy-based electret, better understanding of the factors that govern the performance of the electret, and more detailed electrical characterization of the electret. In particular, the activation energy and time constant of the depoling process can be investigated [33]. Moreover, the electret effect may be improved by using other types of epoxy. An epoxy that has a relatively long molecular structure may be attractive, as it will lower the crosslinking density in the cured epoxy, thereby increasing the mobility of the ions. However, such an epoxy has the disadvantage that it has a relatively high viscosity.

**Acknowledgements** Funding from Mark Diamond Research Fund, University at Buffalo, State University of New York, is gratefully acknowledged. Samples of epoxy and curing agent were kindly provided by Resolution Performance Products (Houston, TX) and BASF Corporation (Florham Park, NJ), respectively.

## References

1. Hsieh WH, Hsu TY, Tai YC (1997) *Transducers* 97:1425
2. Thielemann C, Hess G (1999) In: *Proceedings of SPIE – The International Society for Optical Engineering*, vol 3680. Design,



- test and microfabrication of MEMS and MOEMS. SPIE, pp 748–756
3. Zou Q, Tan Z, Wang Z, Pang J, Qian X, Zhang Q, Lin R, Yi S, Gong H, Liu L, Li Z (1998) *J Microelectromech Syst* 7:224
  4. Gaynor PT, Hughes JF (1998) *Med Biol Eng Comput* 36:615
  5. Shumakov VI, Chepurov AK, Kazlove VK, Kazakova TI (1975) *Polim Med* 5:247
  6. Scott JF, Zubko P (2005) In: Proceedings of the 12th international symposium on electrets (ISE 12), 11–14 Sep 2005, Salvador, Brazil. IEEE, pp 113–115
  7. Magerramov AM, Kerimov MK, Hamidov EM (2004) In: Radiation safety problems in the Caspian region. NATO science series, IV: earth and environmental sciences, vol 41. Springer, The Netherlands, pp 205–209
  8. Bauer S, Bauer-Gogonea S, Dansachumler M, Graz I, Leonhartsberger H, Salhofer H, Schwoediauer R (2003) In: Proceedings of the IEEE ultrasonics symposium, vol 1. IEEE, pp 370–376
  9. Sahu DK, Khare PK, Shrivastava RK (2004) *Indian J Phys* 78:1205
  10. Khare PK, Sahu DK, Verma A, Srivatava RK (2004) *Indian J Pure Appl Phys* 42:693
  11. Fedosov SN, Sergeeva AV, Giacometti JA, Ribeiro PA (1999) In: Proceedings of SPIE – The International Society for Optical Engineering, vol 4017. Polymers and liquid crystals. SPIE, pp 53–58
  12. Holstein P, Leister N, Weber U, Geschke D, Binder H, Monti GA, Harris RK (1999) In: Proceedings of the 10th international symposium on electrets (ISE 10), Delphi, 22–24 Sept 1999, Greece. IEEE, pp 509–512
  13. Eisenmenger W, Schmidt H, Dehlen B (1999) *Braz J Phys* 29:295
  14. Frensch H, Wendorff JH (1985) In: Proceedings of the 5th international symposium on electrets (ISE 5), 1985. IEEE, pp 132–137
  15. Sessler GM, Gerhard-Mulhaupt R, Von Seggern H (1985) In: Proceedings of the 5th international symposium on electrets (ISE 5), 1985. IEEE, pp 565–570
  16. Mellinger A, Singh R, Wegener M, Wirges W, Suarez RF, Lang SB, Santos LF, Gerhard-Mulhaupt R (2005) In: Proceeding of the 12th international symposium on electrets (ISE 12), 11–14 Sept 2005, Salvador, Brazil. IEEE, pp 212–215
  17. Gol'tsov YI, Kramarenko IS, Panchenko EM, Zagoruiko VA, Mal'tsev VT, Sokolova TV (1983) USSR Avail VINITI Deposited Doc, (VINITI 2386-83), 19 pp
  18. Gubkin AN, Popova OS, Ogloblin VA, Kuskova AM (1974) In: Sb Ref –Vses Konf “Fiz Dielektir Perspekt Ee Razvit”, Meeting Date 1973, pp 2126–2127
  19. Gubkin AN, Kashtanova AM, Ogloblin VA, Rastorgueva AV (1972) *USSR Tr Mosk Inst Elektron Mashinostr* 21:38
  20. Nakamura S, Ueshima M, Kobayashi T, Yamashita K (2003) *Key Eng Mater* 240–242 (Bioceramics) 445
  21. Gerhard-Mulhaupt R, Kunstler W, Gome T, Pucher A, Weinhold T, SEIB M (2000) *IEEE Trans Dielectr Electr Insul* 7:480
  22. Mellinger A, Gonzalez FC, Gerhard-Mulhaupt R, Santos LF, Faria RM (2002) In: Proceedings of the 11th international symposium on electrets (ISE 11), 1–3 Oct 2002, Melbourne, Australia. IEEE, pp 7–10
  23. Krashennikov AI, Lipaev SM, Rybnikov YS, Sbrodova LI (1986) *USSR, Lakokrasochnye Materialy i Ikh Primenenie* 3:38
  24. Lee H, Neville K (1957) *Epoxy resins*, Ch. 2. McGraw-Hill Book Company, New York
  25. Peters ST (ed) (1998) *Handbook of composites*, Ch. 2. Chapman and Hall, New York
  26. “Practical use of anhydrous  $\text{LiClO}_4$  and  $\text{Mg}(\text{ClO}_4)_2$  in organic synthesis”, GFS Chemicals Inc, 2002, Issue No. 1, <http://www.gfschemicals.com>, as on Aug 24, 2007
  27. Silva MM, Nunes SC, Barbosa PC, Evans A, de Zea Bermudez V, Smith MJ, Ostrovskii D (2006) *Electrochim Acta* 52:1542
  28. Santhosh P, Vasudevan T, Gopalan A, Lee K-P (2006) *Mater Sci Eng B* 135:65
  29. Wu C-G, Wu C-H, Lu M-I, Chuang H-J (2006) *J Appl Polym Sci* 99:1530
  30. Wegener M, Gerhard-Mulhaupt R (2003) *IEEE Trans Ultrason Ferroelectr Frequency Control* 50:921
  31. Koh WH, Park IH (2003) *J Korean Phys Soc* 42:S920
  32. Nishimura Y (1999) U.S. Patent 5951959
  33. Fedosov SN, Sergeeva AE (1993) *J Electrostat* 30:327